photonics

MDPI

Communication

Study on the Generation of 1.9 μm Mode Superposition Conversion Laser by Double-End Off-Axis Pumping

Chao Li [1], Xinyu Chen [1,*], Ye Sun [1], Jingliang Liu [1,*] and Guangyong Jin [1,2]

[1] Jilin Key Laboratory of Solid Laser Technology and Application, College of Physics, Changchun University of Science and Technology, Changchun 130022, China
[2] College of Material Science and Engineering, Changchun University of Technology, Changchun 130012, China
* Correspondence: 2010800009@cust.edu.cn (X.C.); 2019800023@cust.edu.cn (J.L.)

Abstract: In this paper, the Laguerre–Gaussian (LG) mode superposition is obtained by using the technology of double-end off-axis pumping Tm:YLF crystal, and the LG mode superposition is achieved by combining the extra-cavity conversion method. The impact of changing the off-axis distance on the order of Hermite–Gaussian (HG) mode and the topological charge of LG mode is studied. The results show that when the off-axis distance of the pump source at both ends is tuned, when the off-axis distance is in the range of 260 μm~845 μm, the single-ended 0~10 order HG mode can be obtained. Subsequently, the mode converter is placed to obtain the LG mode beam, and the double-end simultaneously pumps the crystal to obtain the superimposed LG mode. The tuning off-axis quantity changes the topological charge number. When P = 0, $l_1 = l_2$, the superimposed LG mode is a single-ring spot, and the vortex beam center's dark hollow area increases with the topological charge number. When P = 0, $l_1 = -l_2$, the superimposed LG mode is a petal-like spot. The number of petals differs from the topological charges of two opposite numbers. Finally, in the case of changing the topological charge number of the double-ended LG mode, the output of the vortex array structured beams of the tuning mode order 1.9 μm Tm:YLF is completed in the case of conversion and superposition.

Keywords: Hermite–Gaussian mode; topological charge; Laguerre–Gaussian mode; off-axis superposition

Citation: Li, C.; Chen, X.; Sun, Y.; Liu, J.; Jin, G. Study on the Generation of 1.9 μm Mode Superposition Conversion Laser by Double-End Off-Axis Pumping. *Photonics* **2024**, *11*, 210. https://doi.org/10.3390/photonics11030210

Received: 25 January 2024
Revised: 19 February 2024
Accepted: 19 February 2024
Published: 26 February 2024

1. Introduction

Vortex beams carry orbital angular momentum (OAM), also called OAM beams [1]. The phase wavefront is spirally distributed, and this spiral phase structure makes the beam rotate around the center of the beam during propagation. The phase wavefront is spirally distributed, and this spiral phase structure causes the beam to rotate around the center of the beam during propagation. It has a higher degree of spatial freedom and can carry additional information [2]. This feature allows the vortex beam to have a wide range of applications in optical tweezer technology [3,4], quantum optics [5], super-resolution imaging [6], optical communication [7,8], and other fields. The 1.9 μm band has low dispersion and attenuation and can achieve longer distance optical communication transmission. The 1.9 μm laser technology combined with vortex light can improve the information transmission capacity, channel security, and anti-atmospheric attenuation ability, and has the advantage of flexibility. Compared with the water absorption peak at 3 μm [9,10], the 1.9 μm band is more suitable for applications such as optical communication. With the increasing demand for large-capacity optical communication, researchers have gradually turned their attention from a single vortex beam to a composite vortex beam [11,12].

At present, the methods of obtaining the Laguerre–Gaussian (LG) mode are mainly divided into direct and indirect methods. The direct method generally uses a spatial light modulator (SLM) [13–16], spiral phase plate (SPP) [17], and digital micromirror device

(DMD) [18,19]. The indirect method combines the astigmatic mode converter (AMC) [20,21] to obtain the LG mode vortex beam. In 2011, Pravin Vaity et al. [22] used an SLM to generate two coaxial LG mode vortex beams and achieved a maximum of seven-order LG mode superposition output spots. In 2012, D. Naidoo et al. [23] used the intracavity mode selection method to generate two Laguerre–Gaussian beams with different topological charges by SLM and achieved a petal-shaped spot under the superposition of LG modes within eight orders. In 2020, Mateusz Szatkowski et al. [24] used an SLM to superimpose two LG modes of different orders and finally achieved the superposition of $LG_{0,4}$ + $LG_{0,-9}$ modes. In 2018, Shen et al. [25] realized the Hermite–Gaussian (HG) mode within 15 orders through dual off-axis pumping technology and combined it with an AMC to complete LG mode conversion. In the same year, Huang et al. [26] obtained the $HG_{0,1}$ mode by directly exciting the vortex light in the cavity and obtained the $LG_{0,1}$ mode by rotating the gain medium. In 2019, Robin Uren et al. [27] used a double-end end-pumped technique to produce a high-purity $HG_{0,1}$ mode. Based on this purity mode, the incident angle of the $HG_{0,1}$ mode is 45°, and the spherical mirror astigmatism converter is placed to obtain the $LG_{0,1}$ mode with a purity of 94%. In 2021, Liu et al. [28] discovered the conversion of 20-order HG mode to LG mode based on off-axis pumping technology combined with an astigmatism converter. In 2022, Ding et al. [29] used a matrix laser to pump Yb:YAG/YVO_4 to obtain up to 10 orders of HG mode, and then combined it with an astigmatism converter to realize LG mode. In the same year, Zhao et al. [30] realized a 17-order HG mode and wavelength tuning using a single-ended off-axis pumping method. The 16-order LG mode was achieved by combining the astigmatic converter. In 2023, Sun Ye et al. [31] used off-axis pumping technology to study the influence of single-ended different pump spot radius on the purity change of HG mode and realized the LG mode output within eight orders. In 2022, Liu et al. [32] pumped a Tm:YLF crystal with double-ended off-axis pumping technology and studied the influence of multi-dimensional regulation on the output of superimposed evolutionary structured light in the case of double Ince–Gaussian (IG) even modes. The orthogonal superposition of double $IG^{e}_{p,p}$ modes within 10 orders was realized. Currently, most of the research on LG superposition mode is direct SLM evolution output and ordinary visible light and near-infrared (near 1 μm) laser output, and other extra-cavity conversion output LG mode is generally non-superposition mode laser output. There has been no further study on the LG mode superposition phenomenon change in 2 μm wavelength off-axis pumping technology combined with extra-cavity mode conversion.

This paper mainly discusses the dual-end off-axis pumping 1.9 μm Tm:YLF combined with the extra-cavity mode conversion method to realize the superposition control of LG mode and obtain a new method for generating composite vortex beams. The superposition tuning of the HG mode of the vortex beam is realized in the 1.9 μm band, and the conversion from HG mode to LG mode is completed. By changing the off-axis distance, the spot control of the double LG modes is studied when the radial index is 0 and the topological charge is different.

2. Theoretical Analysis

The solid-state laser can achieve HG mode output by using end-face off-axis pumping technology. $HG_{m,n}$ modes propagate in the Cartesian coordinate system, where m and n denote the order of the modes in the x and y directions, respectively, and the formula can be written as follows [33,34]:

$$HG_{m,n}(x,y,z) = \frac{C^{HG}_{m,n}}{w(z)} \exp\left[-\frac{x^2+y^2}{w^2(z)}\right] H_m\left(\frac{\sqrt{2}x}{w(z)}\right) H_n\left(\frac{\sqrt{2}y}{w(z)}\right) \times \exp\left(-i\frac{z}{z_R}\frac{r^2}{w(z)^2}\right) \exp(i\phi_{HG}) \quad (1)$$

where $C_{m,n}^{HG} = 1/\sqrt{\pi 2^{m+n-1} m!n!}$ is the normalized constant, x and y represent the transverse and longitudinal coordinate positions of the beam on the plane. z is the coordinate along the optical axis; z_R is the Rayleigh length, $z_R = kw_0^2/2 = \pi w_0^2/\lambda$; k is the wavenumber; ϕ_{HG} is the Gouy phase, $\phi_{HG} = (m+n+1)arctan(z/z_R)$; $w(z)$ is the beam radius at distance z, $w(z) = \omega_0\left[1+(z/z_R)^2\right]^{1/2}$; and ω_0 is the waist radius of the beam.

To realize the superposition of the double-end off-axis pumping mode, the superimposed *HG* mode is:

$$HG_{superposition} = HG_{m_1,\, n_1}(x, y,\, z) + HG_{m_2,\, n_2}(x, y,\, z)\exp(i\phi_{HG}) \tag{2}$$

After completing the output of the HG mode beam, the mode is converted to obtain the $LG_{p,l}$ mode. The $LG_{p,l}$ mode is the orthogonal solution of the paraxial wave equation in the cylindrical coordinate system. The expression is [35]:

$$\begin{aligned} LG_{p,l}(r,\theta,z) = {} & \frac{C_{p,\updownarrow}^{LG}}{w(z)}\left(\frac{\sqrt{2}r}{w(z)}\right)^{|\updownarrow|}\exp\left(-\frac{r^2}{w^2(z)}\right)L_p^{|\updownarrow|}\left(\frac{2r^2}{w^2(z)}\right)\exp(-i\updownarrow\phi_{LG}) \\ & \times\exp\left(-i\frac{z}{z_R}\frac{r^2}{w(z)^2}\right)\exp(i\phi_{LG}) \end{aligned} \tag{3}$$

In the formula, $C_{l,p}^{LG} = \sqrt{2p!/[\pi(p+|\updownarrow|)!]}$ is the normalized constant; r and θ are the radial and angular coordinates in the cylindrical coordinate system; z is the coordinate along the optical axis; z_R is the Rayleigh length, $z_R = kw_0^2/2 = \pi w_0^2/\lambda$; k is the wavenumber; ϕ_{LG} is the Gouy phase, $\phi_{LG} = (2p+|l|+1)arctan(z/z_R)$; $w(z)$ is the beam radius at distance z, $w(z) = \omega_0\left[1+(z/z_R)^2\right]^{1/2}$; ω_0 is the beam waist radius; l is the angular index (or the number of topological charges); and p is the radial index (or radial node number). When $p = 0$, the $LG_{p,l}$ mode vortex beam spot is a single ring; when $p > 0$, the $LG_{p,l}$ mode vortex beam spot is multi-ring. When $l = 0$, there is no hollow phenomenon. When $l > 0$, there is a hollow phase singularity, and the hollow area increases with the increase l.

So, the superimposed *LG* mode can be written as follows [36]:

$$LG_{superposition} = LG_{p_1,\, l_1}(r, \theta,\, z) + LG_{p_2,\, l_2}(r, \theta,\, z)\exp(i\phi_{LG}) \tag{4}$$

As shown in Figure 1, when the horizontal and vertical directions of the single-ended HG mode are of the same order, the vortex array structured beams are generated by orthogonal superposition. Tuning the order of HG mode can realize the phase singularity change of vortex array structured beams. Then, through the mode conversion of the astigmatic converter, the $LG_{superposition}$ mode with equal topological charge superposition in the horizontal and vertical directions is obtained.

By changing the topological charge number after the superposition of the double LG modes, the obtained mode spot is shown in Figure 2. It can be seen in the figure that in the superimposed LG mode, two equal topological charges or two opposite topological charges can achieve vortex beam control. This superposition mode provides the possibility to expand the capacity of space optical communication and assists in the expansion and deepening of application fields such as space optical communication. Next, the dual-end off-axis pumping technology is used to experimentally complete the HG mode superposition, combined with the conversion of LG mode superposition and tuning order to achieve 1.9 μm laser evolution output.

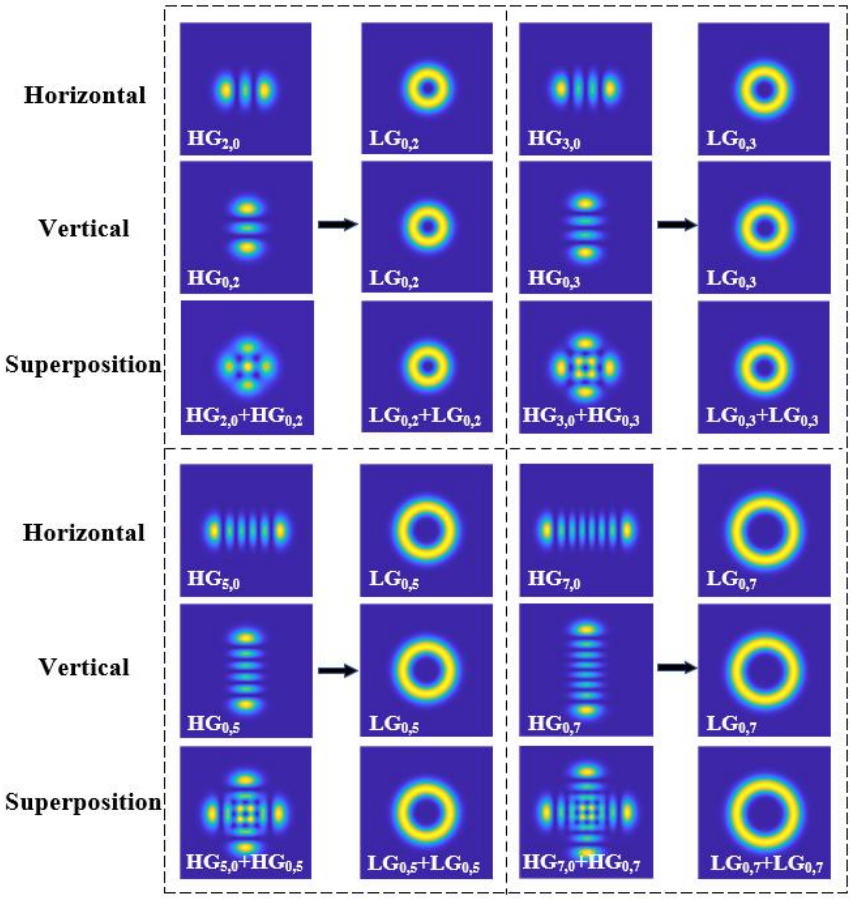

Figure 1. When the $HG_{m,n}$ mode is converted to the $LG_{p,l}$ mode, the two ends are superimposed and tuned to the same order.

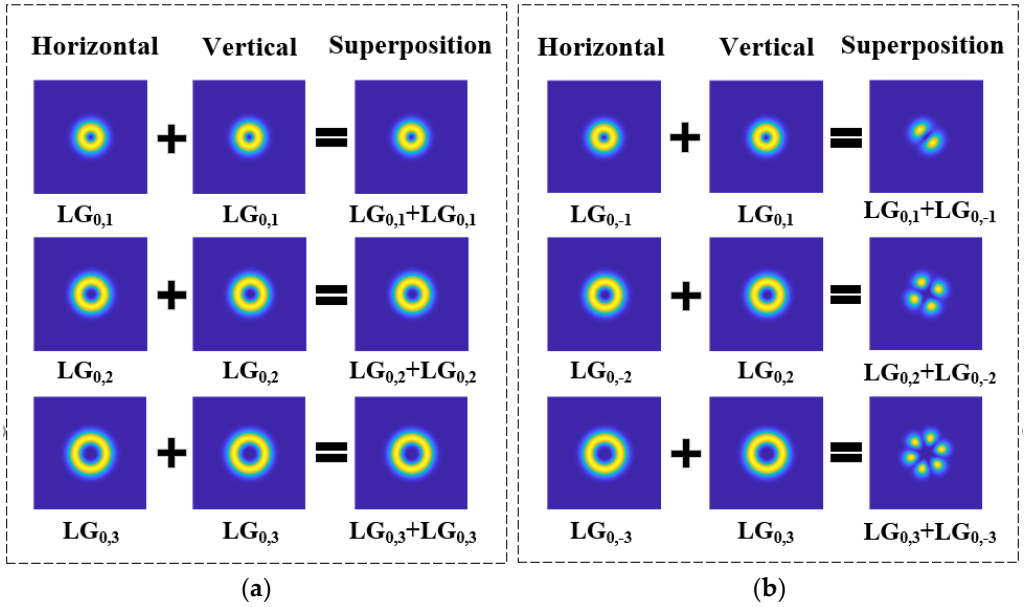

Figure 2. (**a**) superposition when P = 0, $l_1 = l_2$. (**b**) superposition when P = 0, $l_1 = -l_2$.

3. Experimental Apparatus and Results

The experiment uses two Laser Diode (LD) pump sources with an output wavelength of 792 nm. The fiber radius of the pump source is 200 μm and the numerical aperture is 0.22. In the barrel, two lenses are used to form a coupling lens group. The focal length

ratio of the focusing lens group is 40:40, and the pump beam with a spot radius of 200 μm passes through the coupling lens group and enters the crystal. The Tm:YLF crystal with a doping concentration of 3.0 at. % and a-axis cutting is used as the gain medium. The crystal size is 3 × 3 × 14 mm, and its two ends are coated with a laser resistance film with a wavelength of 1.9 μm and a pump high permeability film with a wavelength of 792 nm. Then, the indium foil is wrapped in the crystal and placed on the crystal clip of the external water-cooled tube. At this time, the cooling temperature of the water cooler is 17 °C. The laser resonant cavity is designed as an L-shaped plano-concave cavity. The incident side of the cavity features a total mirror (M2) with a 792 nm attenuated reflection coating (AR) that has a reflection of less than 0.2%. On the output side, there is a highly reflective coating (HR) with a wavelength of 1910 nm and a reflection of over 99.8%. Both the total mirror and the 45° mirror (M1) within the cavity employ the same film system. The Output Coupler (OC) is a mirror for laser output with a transmittance (T) of 5% (R = 300 mm). The overall resonant cavity length is 90 mm, where the distance from the total mirror to the front face of the crystal is 13 mm, the distance from the back face of the crystal to the dichroic mirror (M1) is 13 mm, and the distance from the dichroic mirror to the output coupling mirror is 50 mm. Off-axis pumping is achieved by moving the pumps at both ends horizontally and vertically. A 1908 nm focusing lens (F1) with a focal length of f = 100 mm and an astigmatic mode converter composed of two rows of lenses (f = 25 mm) are placed at the back end of the off-axis pump to generate LG mode beams. In order to fulfill the condition of obtaining the converted mode beam between the two column lenses, the distance between the two column lenses can be obtained as 35.35 mm by the formula $d = \sqrt{2}f$. Finally, the LG mode beam achieved by the conversion of the HG mode and the astigmatism mode converter generated by the double-end anisotropic off-axis pump superposition is observed and recorded by the CCD camera. The experimental setup is shown in Figure 3.

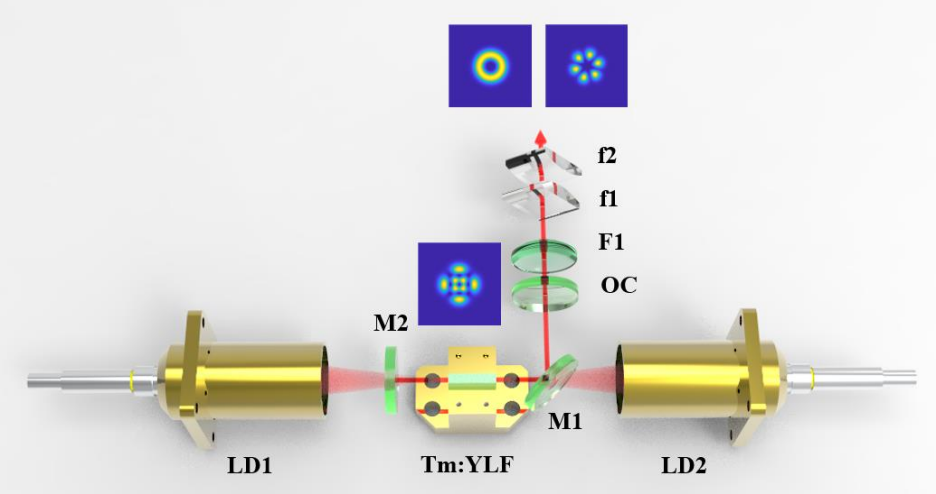

Figure 3. Diagram of the experimental setup for double-ended anisotropic off-axis pumping superposition mode conversion.

Based on the above experimental design, the micrometer knobs on the precision adjustment frame of two load-bearing coupling mirror barrels are rotated, respectively. When a single-ended pump generates a horizontal HG mode beam and rotates a micrometer knob in the horizontal direction, the off-axis distance of the horizontal HG mode can be changed, thereby changing the off-axis distance. Similarly, the same operation is performed in the vertical direction, so that the two generated HG beams are orthogonally superimposed, and their angle is kept unchanged at 90°. The single-ended off-axis pumping HG mode in the horizontal direction and the vertical direction are measured, respectively. On the basis of this mode output, an astigmatic converter is placed to adjust the pump power and

off-axis distance to achieve 0-order to 10-order mode output in the horizontal and vertical directions of the LG mode.

It can be seen from Figure 4 that by adjusting the off-axis distance, the mode order changes, and the tuning output of HG mode and LG mode from 1-order to 10-order is realized. As the number of topological charges in the vortex beam field increases, its chiral structure becomes more complex. In the optical system, there is a difference in the excitation off-axis distance between the fundamental mode and the higher-order modes, where the excitation off-axis distance from the basic mode to the first-order mode is much larger than that of the other modes. Since the fundamental mode has a more excellent range of stable gain in the resonant cavity, it is excited more easily. And as the mode order increases, the off-axis distance gradually decreases, which means that higher-order modes cannot be clearly distinguished. The beams of different orders generated by the orthogonal superposition of two-end mode vortex beams can be seen in Figure 5.

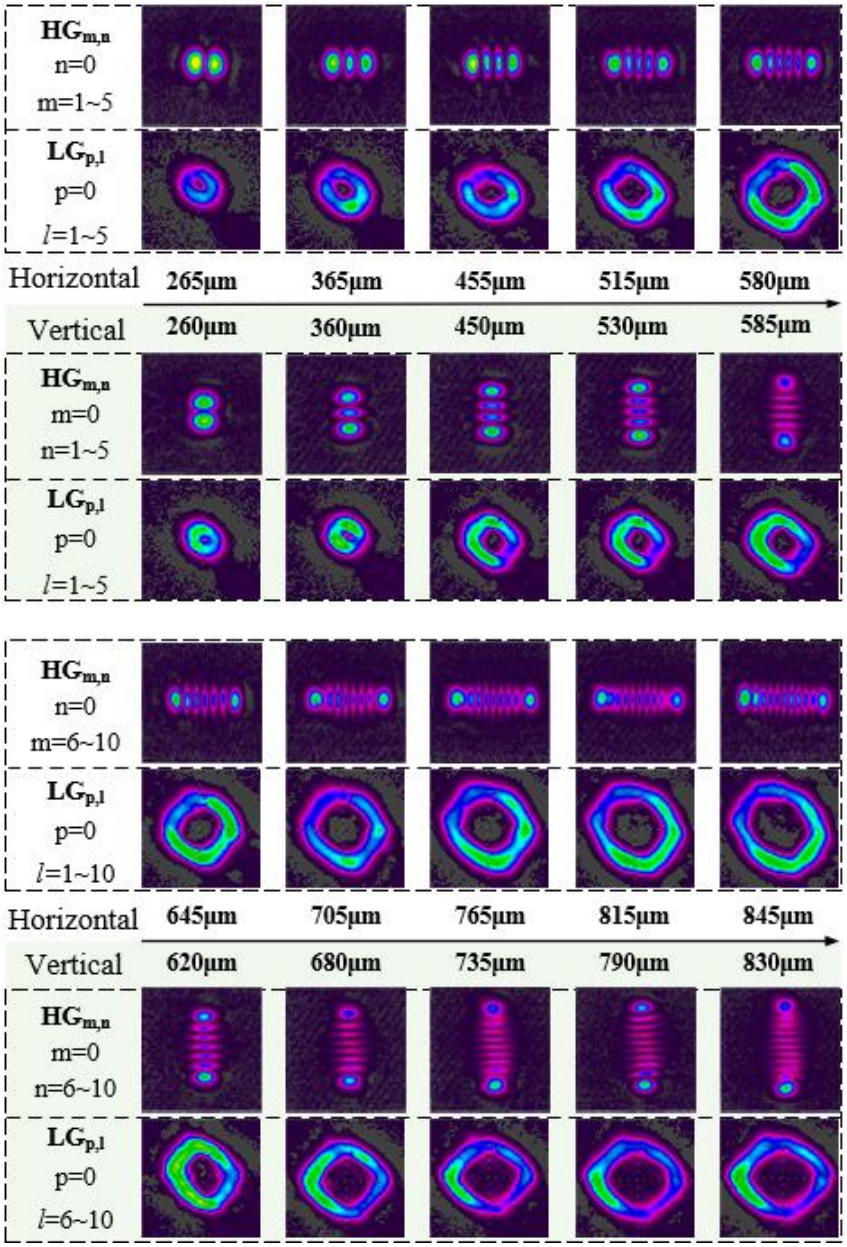

Figure 4. Off-axis quantities for different orders of conversion from HG mode to LG mode for single-ended horizontal and vertical directions.

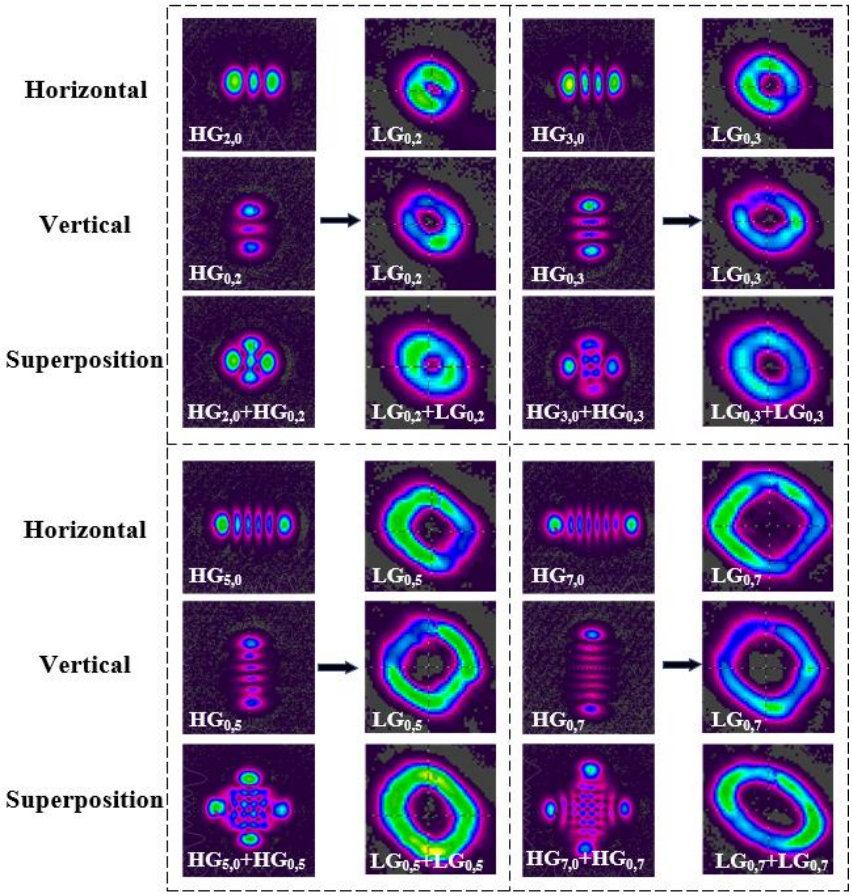

Figure 5. Conversion process from HG mode to LG mode for the same number of orders.

As shown in Figure 5, the theoretical simulation of mode conversion is experimentally verified when the double-ended mode order is the same. The conversion from vortex array structured light to a vortex beam with a dark hollow structure. The experiment agrees with the theoretical formulation.

After the orthogonal superposition of the mode bipartite ends, the LG superposition mode is generated in a bipartite manner under the action of the astigmatic mode converter. Figure 6a,b show the complete process of the change in the topological charge at both ends of the LG mode in the case of orthogonal superposition after the mode conversion.

The LG mode evolution output is completed with the mode conversion of topological charge numbers 1 to 10. The topological charge numbers in Figure 6a are 1, 2, 3, 5, and 7, respectively. The experimentally generated LG mode spot has a circular shape, and the hollow dark spot region of the circular spot increases as the order rises. The experimental results can be consistent with the simulation results of Figure 2 above, and the change in the order tuning mode is verified.

In order to obtain a double LG mode with opposite topological charge, when the off-axis distance of the single end is changed, the off-axis knob moving along the Y-axis direction is moved to the the-Y-axis direction, so that the LG mode beam rotates, and the beams at both ends are superimposed. The topological charges of the beam modes at the tuning ends are opposite, and a petal-like spot with light and dark is generated, as shown in Figure 6b. $P = 0$, l is 1 and (-1), 2 and (-2), 3 and (-3), 5 and (-5), 7 and (-7), respectively, and the number of petals is 2, 4, 6, 10, and 14, respectively. Through experiments, it was found that the larger the off-axis distance, the higher the number of petals, and the number of petals is the topological charge difference between the two vortex beams. This shows that the number of topological charges is closely related to the off-axis distance.

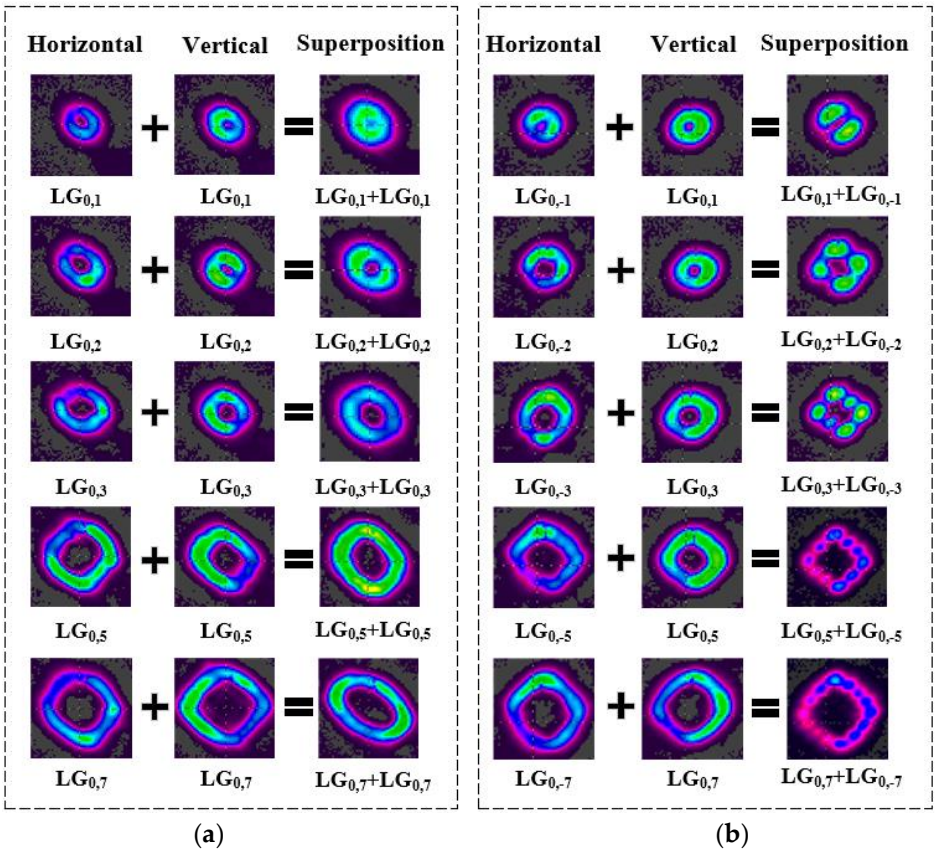

Figure 6. (**a**) Superposition when P = 0, $l_1 = l_2$; (**b**) superposition when P = 0, $l_1 = -l_2$.

4. Conclusions

In summary, the 1.9 μm HG mode is realized in a single simple resonant cavity by using the double-end off-axis pumping Tm:YLF technology. At the same time, combined with the extra-cavity conversion technology, it is converted into the superimposed LG mode and the evolution output of the topological charge number is tuned based on HG mode superposition. In the case of orthogonal superposition, the theoretical simulation and experimental measurement results have a high degree of conformity. The results show that after the superposition of LG modes, the hollow area of the LG mode spot gradually increases when the topological charge numbers are equal at both ends, which are 1, 2, 3, 5, and 7, respectively. The superimposed double LG mode presents a bright and dark petal-like spot when the topological charges at both ends are opposite. This phenomenon shows that the tuning off-axis distance has the ability to regulate the formation of vortex array structured beams. The theoretical and experimental results show that the topological charge of the superposition mode can be tuned when the topological charge of the double LG modes is equal or opposite to each other. In this paper, a new evolutionary output method of 1.9 μm mode superposition conversion with double-end off-axis pumping is realized. It provides a new technical means for the spatial structure tuning of LG mode, which is of great significance for the further development of large-capacity optical communication.

Author Contributions: Conceptualization, C.L. and J.L.; methodology, C.L.; software, C.L. and Y.S.; validation, C.L. and J.L.; formal analysis, C.L.; investigation, C.L.; resources, C.L.; data curation, C.L.; writing—original draft preparation, C.L.; writing—review and editing, C.L.; visualization, C.L.; supervision, X.C.; project administration, X.C. and G.J.; funding acquisition, J.L. All authors have read and agreed to the published version of the manuscript.

Funding: This research was supported by the Project of Jilin Scientific and Technological Development Program (YDZJ202101ZYTS031).

Institutional Review Board Statement: Not applicable.

Informed Consent Statement: Not applicable.

Data Availability Statement: The data that support the findings of this study are available from the corresponding author upon reasonable request.

Conflicts of Interest: The authors declare no conflicts of interest.

References

1. Curtis, J.E.; Grier, D.G. Structure of optical vortices. *Phys. Rev. Lett.* **2003**, *90*, 133901. [CrossRef]
2. Rosales-Guzm'an, C.; Trichili, A.; Dudley, A.; Ndagano, B.; Ben Salem, A.; Zghal, M.; Forbes, A. Optical communications beyond orbital angular momentum. In Proceedings of the Optical Engineering + Applications, San Diego, CA, USA, 28 August–1 September 2016.
3. Simpson, N.B.; Dholakia, K.; Allen, L.; Padgett, M.J. Mechanical equivalence of spin and orbital angular momentum of light: An optical spanner. *Opt. Lett.* **1997**, *22*, 52–54. [CrossRef]
4. Gao, C.; Gao, M.-W.; Weber, H. Generation and application of twisted hollow beams. *Optik* **2004**, *115*, 129–132. [CrossRef]
5. Rjeb, A.; Guerra, G.; Issa, K.; Fathallah, H.A.; Chebaane, S.; Machhout, M.; Palmieri, L.; Galtarossa, A. Inverse-raised-cosine fibers for next-generation orbital angular momentum systems. *Opt. Commun.* **2020**, *458*, 124736. [CrossRef]
6. Tamburini, F.; Anzolin, G.; Umbriaco, G.; Bianchini, A.; Barbieri, C. Overcoming the Rayleigh criterion limit with Orbital Angular Momentum of light. *Phys. Rev. Lett.* **2006**, *97*, 163903. [CrossRef]
7. Xie, Z.; Lei, T.; Li, F.; Qiu, H.; Zhang, Z.; Wang, H.; Min, C.; Du, L.; Li, Z.; Yuan, X. Ultra-broadband on-chip twisted light emitter for optical communications. *Light Sci. Appl.* **2018**, *7*, 18001. [CrossRef]
8. Krenn, M.; Fickler, R.; Fink, M.; Handsteiner, J.; Malik, M.; Scheidl, T.; Ursin, R.; Zeilinger, A. Twisted light communication through turbulent air across Vienna. *arXiv* **2014**, arXiv:1402.2602.
9. Mukai, T.; Mukai, S.; Noguchi, K. Is water-ice the carrier of the 3μm-absorption in infrared objects? *Astrophys. Space Sci.* **1978**, *53*, 77–84. [CrossRef]
10. Esterowitz, L.; Hoffman, C.A. Laser-Tissue/Water Interaction of the Erbium 2.9 μm Laser. In Proceedings of the Cambridge Symposium-Fiber/LASE '86, Cambridge, MA, USA, 18–26 August 1986.
11. Wang, J. Advances in communications using optical vortices. *Photonics Res.* **2016**, *4*, B14–B28. [CrossRef]
12. Willner, A.E.; Huang, H.; Yan, Y.; Ren, Y.; Ahmed, N.; Xie, G.; Bao, C.; Li, L.; Cao, Y.; Zhao, Z.; et al. Optical communications using orbital angular momentum beams. *Adv. Opt. Photonics* **2015**, *7*, 66–106. [CrossRef]
13. Gibson, G.M.; Courtial, J.; Padgett, M.J.; Vasnetsov, M.V.; Pas'ko, V.A.; Barnett, S.M.; Franke-Arnold, S. Free-space information transfer using light beams carrying orbital angular momentum. *Opt. Express* **2004**, *12*, 5448–5456. [CrossRef] [PubMed]
14. Lerner, V.E.; Shwa, D.; Drori, Y.; Katz, N. Shaping Laguerre-Gaussian laser modes with binary gratings using a digital micromirror device. *Opt. Lett.* **2012**, *37*, 4826–4828. [CrossRef]
15. Mirhosseini, M.; Magaña-Loaiza, O.S.; Chen, C.; Rodenburg, B.; Malik, M.; Boyd, R.W. Rapid generation of light beams carrying orbital angular momentum. *Opt. Express* **2013**, *21*, 30196–30203. [CrossRef] [PubMed]
16. Wang, Z.; Yan, Y.; Arbabi, A.; Xie, G.; Liu, C.; Zhao, Z.; Ren, Y.; Li, L.; Ahmed, N.; Willner, A.J.; et al. Orbital angular momentum beams generated by passive dielectric phase masks and their performance in a communication link. *Opt. Lett.* **2017**, *42*, 2746–2749. [CrossRef] [PubMed]
17. Beijersbergen, M.W.; Coerwinkel, R.P.C.; Kristensen, M.; Woerdman, J.P. Helical-wavefront laser beams produced with a spiral phaseplate. *Opt. Commun.* **1994**, *112*, 321–327. [CrossRef]
18. Ren, Y.; Li, M.F.; Huang, K.; Wu, J.; Gao, H.; Wang, Z.; Li, Y.-m. Experimental generation of Laguerre-Gaussian beam using digital micromirror device. *Appl. Opt.* **2010**, *49*, 1838–1844. [CrossRef]
19. Chen, Y.; Fang, Z.-X.; Ren, Y.; Gong, L.; Lu, R. Generation and characterization of a perfect vortex beam with a large topological charge through a digital micromirror device. *Appl. Opt.* **2015**, *54*, 8030–8035. [CrossRef]
20. Beijersbergen, M.W.; Allen, L.; Veen, H.E.L.O.v.d.; Woerdman, J.P. Astigmatic laser mode converters and transfer of orbital angular momentum. *Opt. Commun.* **1993**, *96*, 123–132. [CrossRef]
21. Abramochkin, E.G.; Volostnikov, V.G. Beam transformations and nontransformed beams. *Opt. Commun.* **1991**, *83*, 123–135. [CrossRef]
22. Vaity, P.; Singh, R.P. Self-healing property of optical ring lattice. *Opt. Lett.* **2011**, *36*, 2994–2996. [CrossRef]
23. Naidoo, D.; Ait-Ameur, K.; Brunel, M.; Forbes, A. Intra-cavity generation of superpositions of Laguerre–Gaussian beams. *Appl. Phys. B* **2012**, *106*, 683–690. [CrossRef]
24. Szatkowski, M.; Masajada, J.; Augustyniak, I.; Nowacka, K. Generation of composite vortex beams by independent Spatial Light Modulator pixel addressing. *Opt. Commun.* **2020**, *463*, 125341. [CrossRef]
25. Shen, Y.; Meng, Y.; Fu, X.; Gong, M. Wavelength-tunable Hermite-Gaussian modes and an orbital-angular-momentum-tunable vortex beam in a dual-off-axis pumped Yb: CALGO laser. *Opt. Lett.* **2018**, *43*, 291–294. [CrossRef]
26. Huang, X.; Xu, B.; Cui, S.; Xu, H.; Cai, Z.; Chen, L. Direct Generation of Vortex Laser by Rotating Induced Off-Axis Pumping. *IEEE J. Sel. Top. Quantum Electron.* **2018**, *24*, 1601606. [CrossRef]

27. Uren, R.; Beecher, S.J.; Smith, C.R.; Clarkson, W.A. Method for Generating High Purity Laguerre–Gaussian Vortex Modes. *IEEE J. Quantum Electron.* **2019**, *55*, 1700109. [CrossRef]
28. Liu, J.-L.; Lin, J.; Chen, X.-y.; Yu, Y.; Wu, C.; Jin, G. A 1.9 μm Tm: YLF external cavity mode conversion vortex laser based on LD off-axis pump. *Opt. Commun.* **2021**, *482*, 126596. [CrossRef]
29. Ding, Y.; Yang, J.; Chen, D.; Dong, J. Rectangular Beam Pumped Raman Microchip Laser for Generating Multiwavelength High-Order Hermite–Gaussian Lasers and Vortex Lasers. *Ann. Der Phys.* **2022**, *534*, 2200095. [CrossRef]
30. Zhao, X.; Liu, J.-L.; Liu, M.; Li, R.; Zhang, L.; Chen, X.-Y. An Orbital-Angular-Momentum- and Wavelength-Tunable 2 μm Vortex Laser. *Photonics* **2022**, *9*, 926. [CrossRef]
31. Sun, Y.; Liu, J.-L.; Li, C.; Zhao, X.; Chen, X. Study on the effect of pump beam on the purity of high-order HG mode in off-axis pumped Tm: YLF laser. *Infrared Phys. Technol.* **2023**, *135*, 104954. [CrossRef]
32. Chen, X.-Y.; Yang, X.-N.; Chen, B.; Liu, J.-L. Study on 1.9 μm structured lasers based on Ince–Gaussian modes superposition with multi-modulation by different directions off-axis dual-end-pump. *Opt. Commun.* **2022**, *530*, 129020. [CrossRef]
33. Pratesi, R.; Ronchi, L.A. Generalized Gaussian beams in free space. *J. Opt. Soc. Am.* **1977**, *67*, 1274–1276. [CrossRef]
34. Kotlyar, V.V.; Kovalev, A.A. Hermite-Gaussian modal laser beams with orbital angular momentum. *J. Opt. Soc. Am. A Opt. Image Sci. Vis.* **2014**, *31*, 274–282. [CrossRef]
35. Ando, T.; Matsumoto, N.; Ohtake, Y.; Takiguchi, Y.; Inoue, T. Structure of optical singularities in coaxial superpositions of Laguerre-Gaussian modes. *J. Opt. Soc. Am. A Opt. Image Sci. Vis.* **2010**, *27*, 2602–2612. [CrossRef] [PubMed]
36. Anguita, J.A.; Herreros, J.; Djordjevic, I.B. Coherent Multimode OAM Superpositions for Multidimensional Modulation. *IEEE Photonics J.* **2014**, *6*, 7900811. [CrossRef]